Numerical thermofluid modeling of high-power high-pressure thermal plasma using reaction kinetics

Yasunori Tanaka
Kanazawa University
JAPAN
tanaka@ee.t.kanazawa-u.ac.jp
http://www.ee.t.kanazawa-u.ac.jp/staffs/tanaka/

Introduction-1 :Features of high-pressure plasmas

High-pressure plasmas for materials processing

1. Thermally non-equilibrium plasmas
(ex.Atmospheric-pressure glow discharges APGD, DBD)
- -*Te* >> *T*h
- -**Electron-molecule interactions** are dominant to produce ions & radicals.
- -Gradients of gas density and gas temperature are low.


APGD

2. High power-density plasmas (Thermal plasmas /Meso-plasmas)
~10 MW/m³
- -*Te* ~ *Th* or *Te* > *Th*
- -**Electron-molecule, electron-atom** and **heavy particle-heavy particle interactions** are important to produce ions & radicals
- -**High dissociation degree of gases and highly non-uniform** gas composition can be seen.
- -**Gas density has a wide range of the fourth order** (ex. 0.0001 kg/m³ to 1.0 kg/m³) due to high gradient of gas temperature (300 K-10000 K).

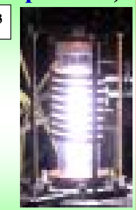

Application of thermal plasmas

Switching devices: HVCB, MCCB

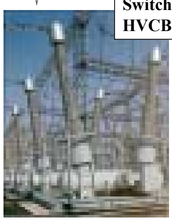
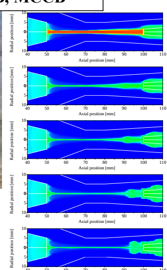

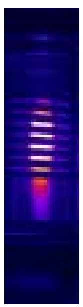

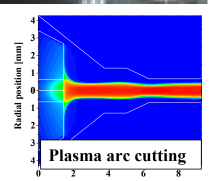

Plasma arc cutting

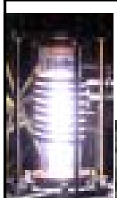
Nanopowder synthesis
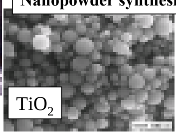

Modulation & Continuous feeding
(80%SCL-PM / CWF)


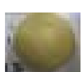
Surface modification

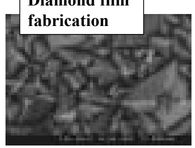
Diamond film fabrication

Introduction-2

Modeling of Thermal Plasmas

The conventional model for thermal plasmas assumes LTE (Local Thermodynamic Equilibrium) condition:

A. Thermal equilibrium
 # All temperatures including *T*e, *T*h, *T*ex, *T*rot, *T*vib, etc are assumed to be the same.

B. Chemical equilibrium
 # Infinite reaction rates for all reactions
→ Reaction field instantaneously reaches its equilibrium.
→ Reaction field is determined only by *T* and *P*.

Actual situations
- -Very high gas flow velocity
- -Rapid change in state (Transient state)
- -Low temp. region⇒Low reaction rate
- -High electric field strength
- -High gradient of particle density

⇨ **Thermally & Chemically Non-Equilibrium Conditions**

Our work that has been done

#1. A chemically non-equilibrium model

#2. A <u>two-temperature chemically non-equilibrium model</u> for thermal plasmas was developed using reaction kinetics.

-Consideration of reaction rates for hundreds of reactions

-Thermodynamic and transport properties were self-consistently calculated using non-CE density and T <u>at each position at each calculation step</u>.

Today's presentation

Results of thermal plasmas with O_2 gas

Pulsed arc discharge in dry air,

$Ar+N_2+O_2$ ICPs,

Dielectric strength of hot air

($Ar+N_2$, $Ar+N_2+H_2$, $Ar+CO_2+H_2$, $Ar+CH_4+O_2$, SF_6 plasmas have been also developed)

-Nanopowder synthesis
-Surface modification
-Syngas production

-Results of temperature fields, particle composition
-Comparison with LTE calculation results

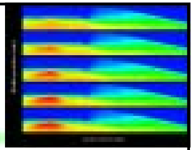

Non-equilibrium modeling of arcs/thermal plasmas

1. ***Chemically non-equilibrium effects***
2. ***Thermally non-equilibrium effects***
3. ***Non-Maxwellian EEDF***

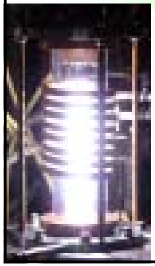

Keywords:
-Chemically non-equilibrium
-Reaction rates
-Convection and diffusion

How to consider chemically non-equilibrium

A conventional model for thermal plasmas ***Te~Th***

Assumption of **local thermodynamic equilibrium (LTE) condition**

→<u>Particle composition</u> can be determined only by local temperature and pressure through the <u>mass action law</u>.

-Solving Saha equations & Guldberg-Waage equations

-Minimization of Gibb's free energy of a system

Actual situations

-Reaction rates are finite → Time scale of a system~Reaction time

-Convection and diffusion effects are not negligible for particle composition determination

Mass conservation of each of species *j*:

$$\frac{\partial(\rho Y_j)}{\partial t}+\nabla\cdot(\rho \boldsymbol{u} Y_j+\boldsymbol{J}_j)=m_j\sum_{\ell=1}^{L}(\beta^r_{j\ell}-\beta^f_{j\ell})\left(\alpha^f_\ell\prod_{i=1}^{N}n_i^{\beta^f_{i\ell}}-\alpha^r_\ell\prod_{i=1}^{N}n_i^{\beta^r_{i\ell}}\right)$$

Convection   Diffusion   Production by reactions

<u>This equation should be solved to determine particle composition considering chemically non-equilibrium effects.</u>

Consideration of chemically non-equilibrium

Mass conservation of species *j*:

$$\frac{\partial(\rho Y_j)}{\partial t}+\nabla\cdot(\rho \boldsymbol{u} Y_j+\boldsymbol{J}_j)=m_j\sum_{\ell=1}^{L}(\beta^r_{j\ell}-\beta^f_{j\ell})\left(\alpha^f_\ell\prod_{i=1}^{N}n_i^{\beta^f_{i\ell}}-\alpha^r_\ell\prod_{i=1}^{N}n_i^{\beta^r_{i\ell}}\right)$$

Convection   Diffusion   Production by reactions

#Disadvantages in treatment of chemically non-equilibrium

(i) <u>A large amount of data concerning reaction rates with a wide temperature range are necessary</u>.

(ii) Thermodynamic and transport properties cannot be calculated in advance as functions of *T* & *P*.

→ <u>They should be calculated at each position with local T & P and particle composition calculated</u>.

(iii) Numerical instability often occurs because of a wide range of reaction rates.

→An implicit method is usually adopted to solve the mass conservation equations.

→ **Examples of chemically non-equilibrium modeling will be presented.**

Y.Tanaka, PSST, 14, 134, 2005

Ex-1. Modelling of pulsed arc discharges in air

Example 1: A pulsed arc discharge in air with I_{peak}=72A, t_f/t_h= 1.0/12 μs.

Simple model

Assumptions

(1) Pressure surrounding the arc is the atmospheric pressure, i.e. 101325 Pa.
(2) The one-temperature model is adopted, i.e. $T=T_e=T_h$.
(3) Axisymmetric structure.
(4) Optically thin.
(5) Turbulence is neglected.
(6) The electric field has only an axial component, while magnetic field has only an azimuthal one.
(7) The dry-air plasma has 13 species: N_2, N_2^+, N, N^+, O_2, O_2^+, O, O^+, NO, NO^+, and e.
(8) Reaction rates depend on Arrehius' law.
(9) Chemically equilibrium(CE) is not dictated.

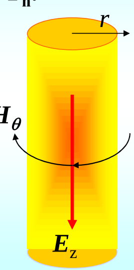

Governing equations

-Mass conservation:

$$\frac{\partial \rho}{\partial t}+\frac{1}{r}\frac{\partial (r\upsilon\rho)}{\partial r}=0$$

-Momentum conservation:

$$\frac{\partial (\rho\upsilon)}{\partial t}+\frac{1}{r}\frac{\partial (r\upsilon\rho\upsilon)}{\partial r}=-\frac{\partial p}{\partial r}+\frac{1}{r}\frac{\partial}{\partial r}\left(2r\eta\frac{\partial \upsilon}{\partial r}\right)-2\eta\frac{\upsilon}{r^2}-\sigma\mu_0E_zH_\theta$$

-Energy conservation:

$$\frac{\partial}{\partial t}\left[\rho(h+\frac{\upsilon^2}{2})\right]+\frac{1}{r}\frac{\partial}{\partial r}\left[r\upsilon\rho(h+\frac{\upsilon^2}{2})\right]$$
$$=\frac{1}{r}\frac{\partial}{\partial r}\left(r\frac{\kappa}{C_{pm}}\frac{\partial h}{\partial r}\right)+\frac{1}{r}\frac{\partial}{\partial r}\left(r\sum_{j=1}^{N}\left(\rho D_j-\frac{\kappa}{C_{pm}}\right)\cdot h_j\frac{\partial Y_j}{\partial r}\right)+\sigma E_z^2-P_{rad}$$

-Mass conservation of species *j*:

$$\frac{\partial (\rho Y_j)}{\partial t}+\frac{1}{r}\frac{\partial (r\upsilon\rho Y_j)}{\partial r}-\frac{1}{r}\frac{\partial}{\partial t}\left(r\rho D_j\frac{\partial Y_j}{\partial r}\right)=m_j\sum_{l=1}^{L}\left(\beta_{jl}^r-\beta_{jl}^f\right)\cdot\left(\alpha_l^f\prod_{i=1}^{N}n_i^{\beta_{il}^f}-\alpha_l^r\prod_{i=1}^{N}n_i^{\beta_{il}^r}\right)$$

-Charge neutrality: $n_{e^-}=n_{N_2^+}+n_{N^+}+n_{O_2^+}+n_{O^+}+n_{NO^+}$

-Equation of state: $p=\sum n_jkT$

-Ohm's law: $$E_z=\frac{I}{\int_0^\infty 2\pi\sigma r dr}$$

-Ampere's law: $$H_\theta=\frac{1}{r}\int_0^r \sigma E_z\xi d\xi$$

Solving these eqs. enables one to drive n_j without CE assumption.

t : time, ρ: mass density, r : radial position, υ : radial velocity, p: pressure, σ: electrical conductivity, μ_0: permeability, E_z: electric field strength, H_θ: magnetic field strength, h: enthalpy, κ: thermal conductivity, D_j: effective diffusion coefficient, C_{pm}: effective specific heat, Y_j: mass fraction, P_{rad}: radiation loss, β_{jl}: stoichiometric coefficient, α_l : reaction rate

Reactions in dry-air plasmas

1 : $2O_2 \rightarrow 2O + O_2$
2 : $O_2 + NO \rightarrow 2O + NO$
3 : $O_2 + N_2 \rightarrow 2O + N_2$
4 : $O_2 + O \rightarrow 3O$
5 : $O_2 + N \rightarrow 2O + N$
6 : $NO + O_2 \rightarrow N + O + O_2$
7 : $2NO \rightarrow N + O + NO$
8 : $NO + N_2 \rightarrow N + O + N_2$
9 : $NO + O \rightarrow N + 2O$
10: $NO + N \rightarrow 2N + O$
11: $N_2 + O_2 \rightarrow 2N + O_2$
12: $N_2 + NO \rightarrow 2N + NO$
13: $2N_2 \rightarrow 2N + N_2$
14: $N_2 + O \rightarrow 2N + O$
15: $N_2 + N \rightarrow 3N$
16: $N_2 + e^- \rightarrow 2N + e^-$
17: $N_2 + O \rightarrow NO + N$
18: $NO + O \rightarrow N + O_2$
19: $N + O \rightarrow NO^+ + e^-$
20: $2N \rightarrow N_2^+ + e^-$
21: $2O \rightarrow O_2^+ + e^-$
22: $O + e^- \rightarrow O^+ + 2e^-$
23: $N + e^- \rightarrow N^+ + 2e^-$
24: $NO^+ + O \rightarrow N^+ + O_2$
25: $O_2^+ + N \rightarrow N^+ + O_2$
26: $NO + O^+ \rightarrow N^+ + O_2$
27: $O_2^+ + N_2 \rightarrow N_2^+ + O_2$
28: $O_2^+ + O \rightarrow O^+ + O_2$
29: $NO^+ + N \rightarrow O^+ + N_2$
30: $NO^+ + O_2 \rightarrow O_2^+ + NO$
31: $NO^+ + O \rightarrow O_2^+ + N$
32: $O^+ + N_2 \rightarrow N_2^+ + O$
33: $NO^+ + N \rightarrow N_2^+ + O$
34: $N_2^+ + N \rightarrow N_2 + N^+$
35: $N_2^+ + N_2 + e^- \rightarrow 2N_2$
36: $N_2^+ + N + e^- \rightarrow N_2 + N$
37: $N^+ + N_2 + e^- \rightarrow N + N_2$
38: $N^+ + N + e^- \rightarrow 2N$
39: $O_2 + e \rightarrow 2O + e$
40: $O_2 + e \rightarrow O_2^+ + 2e$
41: $NO + e \rightarrow NO^+ + 2e$
42: $N_2 + e \rightarrow N_2^+ + 2e$

42 forward reactions & their backward reactions

Totally 84 reactions were taken into account

Rate coefficients
-Forward reactions: by Arrhenius law using data of C.Park (NASA)
-Backward reactions: by the principle of detailed balancing

Transport properties of dry-air arc plasmas-1

First order approximation of Chapman-Enskog method

Transport properties

-Electrical conductivity

$$\sigma=\frac{e^2}{kT}\frac{n_e}{\sum_{j\neq e}n_j\Delta_{ej}^{(1)}}$$

-Effective diffusion coefficient

$$D_j=\frac{1-Y_j}{\sum_{i\neq j}\frac{x_i}{D_{ji}}}\qquad D_{ij}=\frac{kT}{p}\frac{1}{\Delta_{ij}^{(1)}}$$

$$\frac{1}{\Delta_{ij}^{(1)}}=\frac{3}{8}\sqrt{\frac{\pi kT(m_i+m_j)}{2m_im_j}}\frac{1}{\pi\overline{\Omega}_{ij}^{(1,1)}}$$

Rapid transient phenomena in pulsed arc discharges
↓
Chemical non-equilibrium

-Thermodynamic and transport properties depends on not only *T* & *p* but also particle composition n_j at each time step at each position.

k :Boltzmann const., T: temperature, e: electronic charge, n_j: density of species j, m_j: mass of species j, $\pi\Omega_{ij}$: collision integral between i-j, x_i:mole fraction of species j, Y_j: mass fraction of species j, p : pressure (Pa)

Transport properties of dry-air arc plasmas-2

Transport properties

-Thermal conductivity

$$\kappa = \frac{15}{4} k \sum_{i=1}^{N} \frac{n_i}{\sum_{j=1}^{N} \xi_{ij} n_j \Delta_{ij}^{(2)}}$$

$$\frac{1}{\Delta_{ij}^{(2)}} = \frac{5}{16} \sqrt{\frac{\pi k T (m_i + m_j)}{2 m_i m_j}} \frac{1}{\pi \overline{\Omega}_{ij}^{(2,2)}}$$

$$\xi_{ij} = 1 + \frac{(1 - m_i / m_j) \cdot (0.45 - 2.54 m_i / m_j)}{(1 + m_i / m_j)^2}$$

-Viscosity

$$\eta = \sum_{j=1}^{N} \frac{m_j n_j}{\sum_{i=1}^{N} n_i \Delta_{ij}^{(2)}}$$

Thermodynamic properties

$$h = \sum_{j=1}^{N} Y_j h_j$$

$$h_j = \frac{1}{m_j} \left(\frac{5}{2} kT + kT^2 \frac{\partial}{\partial T} (\ln Z_j) + \Delta H_{fj} \right)$$

$$C_{pm} = \sum_{j=1}^{N} \left(Y_j \frac{\partial h_j}{\partial T} \right)$$

Z_j: internal partition function of species j,
ΔH_{fj}: standard enthalpy of formation

Electric current waveform

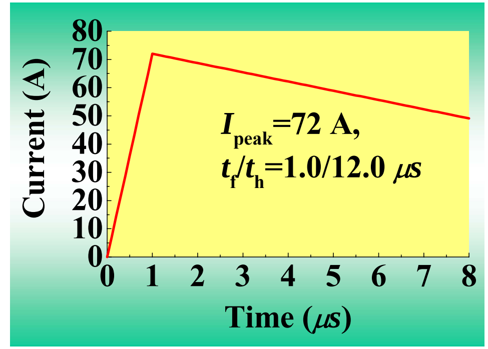

-Peak value of current =72A

-Time duration to peak = 1.0 μs

-Time duration to half current=12.0μs

The similar waveform to that in the experiment was adopted for comparison.

Time evolution in temperature

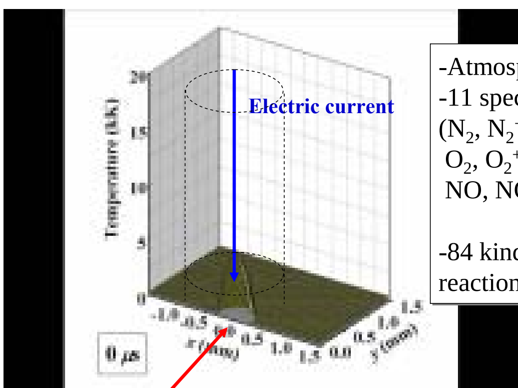

-Atmospheric air
-11 species
(N_2, N_2^+, N, N^+, O_2, O_2^+, O, O^+, NO, NO^+,e)

-84 kinds of reactions

(x, y)=(0,0) : center axis of the arc

An increase in temperature on center axis arises from increasing joule heating there.

Time evolution in pressure

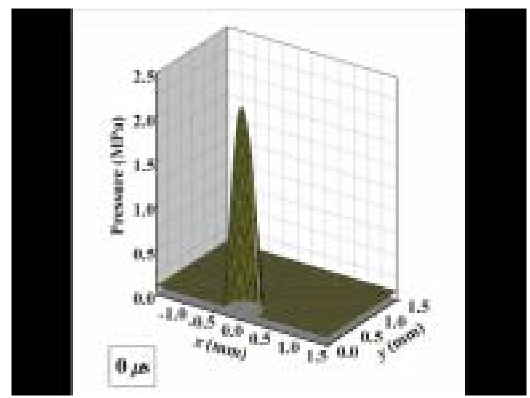

A rapid decrease in pressure around the axis can be seen.
A discontinuous surface is generated → Shock-wave

Time evolution in mass density

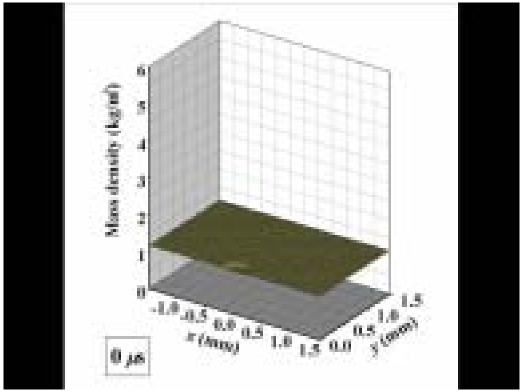

A rapid decrease in ρ around the axis and an increase in ρ surrounding the arc are due to the generated shock-wave.

Time evolution in particle composition distribution

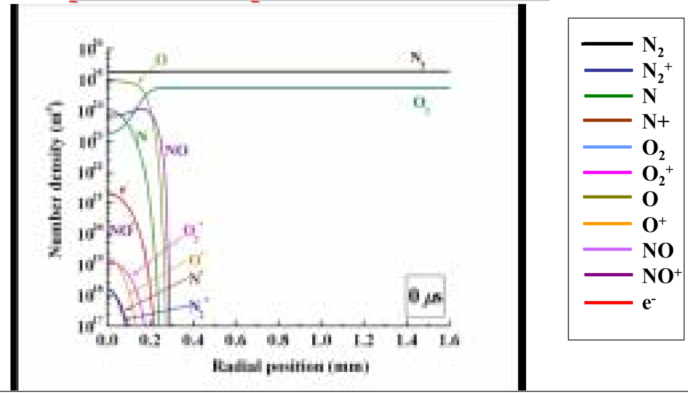

A rapid change in composition arising from dissociation and ionization reactions can be seen until about t=1.0 μs.
From t>1.0 μs, the composition change is due mainly to the radial transport.

Dominant reactions for generation/disappearance of species

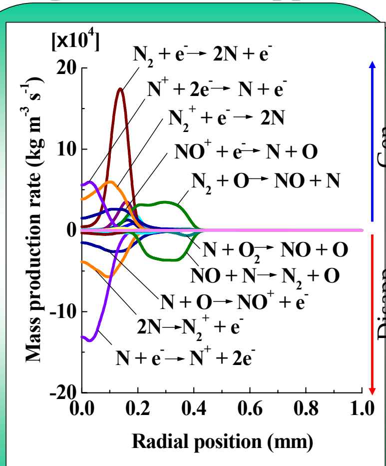

Mass production rate of N atom by each reaction at t=0.4 μs after ignition

Gen.: N_2+e → 2N + e
Disapp.: N+e → N^+ +e

Dominant reactions for generation/disappearance of species at 0.4 μs after arc ignition

	Generation	Disappearance
N_2	$NO + N \rightarrow N_2 + O$	$N_2 + e^- \rightarrow 2N + e^-$
N_2^+	$2N \rightarrow N_2^+ + e^-$	$N_2^+ + e^- \rightarrow 2N$
N	$N_2 + e^- \rightarrow 2N + e^-$	$N + e^- \rightarrow N^+ + 2e^-$
N^+	$N + e^- \rightarrow N^+ + 2e^-$	$N^+ + 2e^- \rightarrow N + e^-$
O_2	$2O + N_2 \rightarrow O_2 + N_2$	$N + O_2 \rightarrow NO + O$
O_2^+	$2O \rightarrow O_2^+ + e^-$	$O_2^+ + e^- \rightarrow 2O$
O	$O^+ + 2e^- \rightarrow O + e^-$	$O + e^- \rightarrow O^+ + 2e^-$
O^+	$O + e^- \rightarrow O^+ + 2e^-$	$O^+ + 2e^- \rightarrow O + e^-$
NO	$N_2 + O \rightarrow NO + N$	$NO + N \rightarrow N_2 + O$
NO^+	$N + O \rightarrow NO^+ + e^-$	$NO^+ + e^- \rightarrow N + O$
e^-	$O + e^- \rightarrow O^+ + 2e^-$ $N + e^- \rightarrow N^+ + 2e^-$	$O^+ + 2e^- \rightarrow O + e^-$ $N^+ + 2e^- \rightarrow N + e^-$

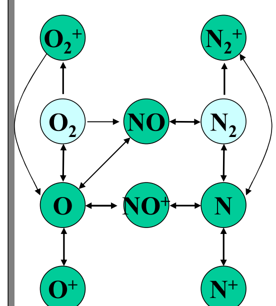

Heavy particle chemistry at t=0.4 μs

Comparison with experimental results-1: Neutral particle density, electron density

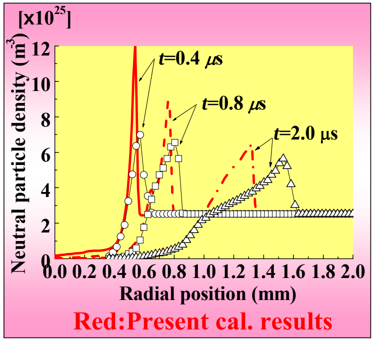

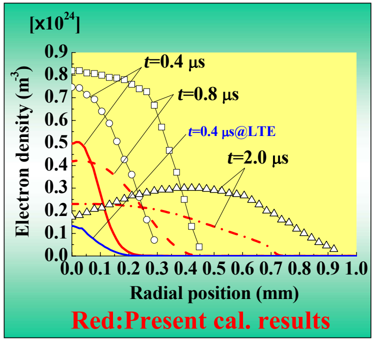

Experimental results were obtained with a two-wavelength laser-interferometer by Akazaki et al.

Good agreements between calculation results and experimental ones.

Comparison with experimental results-2 Arc radius, expanding velocity of shock wave

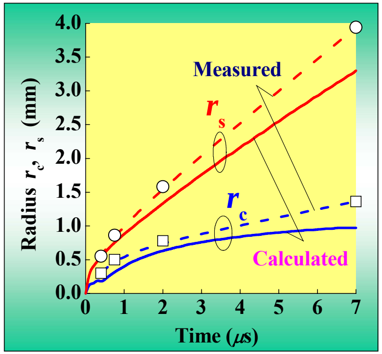

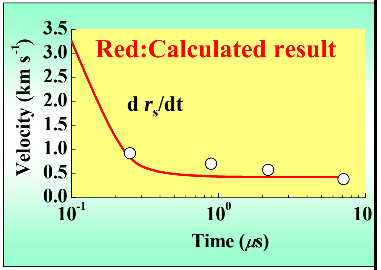

r_s: Radial position of shock wave surface

r_c: Arc channel radius defined as the radius in which 90% electrons is included.

Good agreements between calculation results and experimental ones.

Summary

Development of
1-D Chemical non-equilibrium model of pulsed arc discharges in dry air at atmospheric pressure (84 reactions considered)

Time evolutions in temperature, pressure, mass density, particle composition in a pulsed arc discharge was obtained.
→Shock-wave generation
→Dominant reactions for each particle

Comparison with experimental results:
-Neutral particle density,
-Electron density,
-Arc conducting radius and its expanding velocity,
-Radial position of shock-wave surface and its expanding velocity
→ Good agreements were obtained.

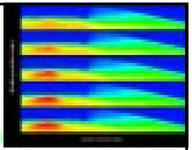

Non-equilibrium modeling of arcs/thermal plasmas

1. *Chemically non-equilibrium effects*
2. *Thermally non-equilibrium effects*
3. *Non-Maxwellian EEDF*

Keywords:
-Chemically non-equilibrium
-Reaction rates
-Convection and diffusion

Cross-section of plasma torch and reactor

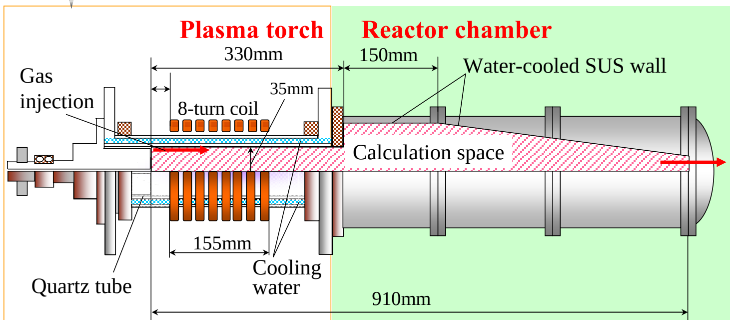

Calculation conditions

Frequency: 450 kHz, RF.Power: **13.5**, 27.0 kW

Pressure: 1, 0.5, **0.3** atm

Gas:Sheath gas Ar/additional gas=98/2 slpm(e.g.)

Additional gas N_2=2, N_2+H_2=1+1, N_2+O_2=1.56+0.44 slpm(air)

2T-NCE Modeling of Ar plasmas with molecular gases

Assumptions

(1) Steady state

(2) Axisymmetric structure

(3) Laminar flow, therefore the turbulent effect is negligible.

(4) Optically thin

(5) *Chemically non-equilibrium condition is allowed.*

(6) *Te* can be different from *Th*

Particles considered

For Ar+N_2+O_2 plasma:

13 species: N_2, N_2^+, N, N^+, O_2, O_2^+, O, O^+, NO, NO^+, Ar, Ar^+, e

Governing equations

-Mass conservation:

$$\frac{\partial \rho}{\partial t} + \nabla \cdot (\rho \boldsymbol{u}) = 0$$

-Equation of state

-Charge neutrality

-Momentum conservation:

Axial:

$$\frac{\partial(\rho u)}{\partial t} + \nabla \bullet (\rho \boldsymbol{u} u) = -\frac{\partial p}{\partial z} + \nabla \bullet (\eta \nabla u) + \nabla \bullet \left(\eta \frac{\partial \boldsymbol{u}}{\partial z}\right) + \mu_0 \sigma \Re\left[\dot{E}_\theta \dot{H}_r^*\right]$$

Radial:

$$\frac{\partial(\rho \upsilon)}{\partial t} + \nabla \bullet (\rho \boldsymbol{u} \upsilon) = -\frac{\partial p}{\partial r} + \nabla \bullet (\eta \nabla \upsilon) + \nabla \bullet \left(\eta \frac{\partial \boldsymbol{u}}{\partial r}\right) - 2\eta \frac{\upsilon}{r^2} + \frac{\rho v w}{r} + \mu_0 \sigma \Re\left[\dot{E}_\theta \dot{H}_z^*\right]$$

Swirl:

$$\frac{\partial(\rho w)}{\partial t} + \nabla \bullet (\rho \boldsymbol{u} w) = \nabla \bullet (\eta \nabla w) + \frac{\rho v w}{r} - \frac{w}{r}\frac{\partial (r\eta)}{\partial r}$$

-Energy conservation for heavy particles:

$$\frac{\partial(\rho h')}{\partial t} + \nabla \bullet (\rho \boldsymbol{u} h') = \nabla \bullet \left(\lambda_{\mathrm{h}}^{\mathrm{tr}} \nabla T_{\mathrm{h}}\right) + \sum_j^N \left[\nabla \bullet \left(\rho D_j h'_j \nabla Y_j\right)\right] - \sum_{\ell(\beta_{\mathrm{e}\ell}^f \cdot \beta_{\mathrm{e}\ell}^r = 0)}^L \Delta Q_\ell + E_{\mathrm{eh}}$$

-Energy conservation for electrons:

$$\frac{\partial}{\partial t}\left(n_{\mathrm{e}} \frac{5}{2} \kappa T_{\mathrm{e}}\right) + \nabla \bullet \left(n_{\mathrm{e}} \boldsymbol{u} \frac{5}{2} \kappa T_{\mathrm{e}}\right) = \nabla \bullet \left(\lambda_{\mathrm{e}}^{\mathrm{tr}} \nabla T_{\mathrm{e}}\right) - \sum_j^N \left[\nabla \bullet \left(\frac{1}{m_{\mathrm{e}}} \frac{5}{2} \kappa T_{\mathrm{e}} \boldsymbol{\Gamma}_{\mathrm{e}}\right)\right] + \sigma E_\theta E_\theta^* - P_{\mathrm{rad}} - \sum_{\ell(\beta_{\mathrm{e}\ell}^f \cdot \beta_{\mathrm{e}\ell}^r \neq 0)}^L \Delta Q_\ell - E_{\mathrm{eh}}$$

Reaction heat

Energy transfer between h & e

-Mass conservation for each particle:

$$\frac{\partial(\rho Y_j)}{\partial t} + \nabla \bullet (\rho \boldsymbol{u} Y_j) = \nabla \bullet (\rho D_j \nabla Y_j) + m_j \sum_l^L \left[\left(\beta_{jl}^r - \beta_{jl}^f\right) \cdot \left(\alpha_l^f \prod_i^N n_i^{\beta_{il}^f} - \alpha_l^r \prod_i^N n_i^{\beta_{il}^r}\right)\right]$$

-Maxwell eq. for vector potential:

$$\nabla^2 \dot{A}_\theta = j\omega\sigma\mu_0 \dot{A}_\theta$$

etc…

Ex.: Reactions in Ar-N_2+O_2 plasma

1: $O_2 + O_2 \rightarrow O + O + O_2$
2: $O_2 + NO \rightarrow O + O + NO$
3: $O_2 + N_2 \rightarrow O + O + N_2$
4: $O_2 + O \rightarrow O + O + O$
5: $O_2 + N \rightarrow O + O + N$
6: $O_2 + Ar \rightarrow O + O + Ar$
7: $NO + O_2 \rightarrow N + O + O_2$
8: $NO + NO \rightarrow N + O + NO$
9: $NO + N_2 \rightarrow N + O + N_2$
10: $NO + O \rightarrow N + O + O$
11: $NO + N \rightarrow N + O + N$
12: $NO + Ar \rightarrow N + O + Ar$
13: $N_2 + O_2 \rightarrow N + N + O_2$
14: $N_2 + NO \rightarrow N + N + O$
15: $N_2 + N_2 \rightarrow N + N + N_2$
16: $N_2 + O \rightarrow N + N + O$
17: $N_2 + N \rightarrow N + N + N$
18: $N_2 + Ar \rightarrow N + N + Ar$
19: $N_2 + e \rightarrow N + N + e$
20: $N_2 + O \rightarrow NO + N$
21: $NO + O \rightarrow N + O_2$
22: $N + O \rightarrow NO^+ + e$
23: $N + N \rightarrow N_2^+ + e$
24: $O + O \rightarrow O_2^+ + e$
25: $O + e \rightarrow O^+ + e + e$
26: $N + e \rightarrow N^+ + e + e$
27: $NO^+ + O \rightarrow N^+ + O_2$
28: $O_2^+ + N \rightarrow N^+ + O_2$
29: $NO + O^+ \rightarrow N^+ + O_2$
30: $O_2^+ + N_2 \rightarrow N_2^+ + O_2$
31: $O_2^+ + O \rightarrow O^+ + O_2$
32: $NO^+ + N \rightarrow O^+ + N_2$
33: $NO^+ + O_2 \rightarrow O_2^+ + NO$
41: $N^+ + N + e \rightarrow N + N$
42: $O_2 + e \rightarrow O + O + e$
43: $O_2 + e \rightarrow O_2^+ + e + e$
44: $NO + e \rightarrow NO^+ + e + e$
45: $N_2 + e \rightarrow N_2^+ + e + e$
46: $Ar^+ + e + e \rightarrow Ar + e$
47: $Ar + Ar \rightarrow Ar^+ + e + Ar$

94 reactions were considered.

Reaction rate coefficients:

#Temperature-dependent approximation

1. Arrhenius type: $\alpha = aT^b \exp(-c/T)$

2. Lennard-Jones type:

$\alpha = a\exp(b + cT + dT^2)\exp(-c/T)$

#. Energy Distribution Function:

$$\alpha_\ell^f = \left(\frac{2e}{m}\right)^{1/2} \int_0^\infty \sigma_\ell(\varepsilon) f(\varepsilon) \varepsilon d\varepsilon$$

Maxwellian for heavy particles

Ex. Rate coefficients of electron impact reactions

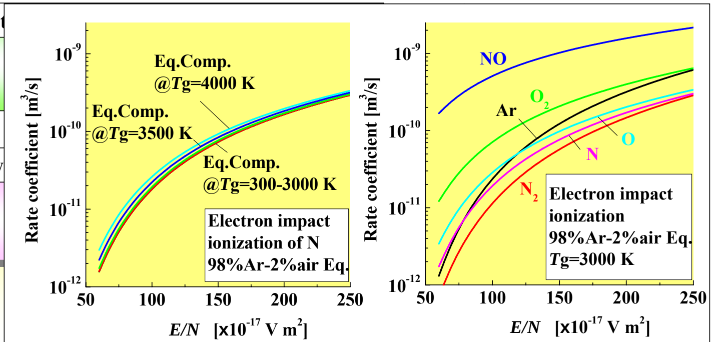

$$J_{\mathrm{el}} = -N\left(\frac{2\varepsilon}{m}\right)^{1/2}\sum_s \delta_s \frac{2m}{M_2}\sigma_e(\varepsilon)\left[n\left(\frac{kT_g}{2}-\varepsilon\right)-kT_g\varepsilon\frac{\partial n}{\partial \varepsilon}\right]$$

: Energy loss in elastic collisions

$$R_{sj}(\varepsilon) = \left(\frac{2}{m}\right)^{1/2}\left[\varepsilon^{1/2}\sigma_{sj}(\varepsilon)\right]$$

Rate of inelastic collisions such as excitation, ionization

$n(\varepsilon) = n_e f_0(\varepsilon)\varepsilon^{1/2}$ **EEDF: Electron energy distribution function**

Transport properties of thermal plasma

Influenced markedly by temperature and composition

Transport and thermodynamic properties for heavy particles and electrons are calculated at each position using non-equilibrium composition and collision integrals.

The first order approximation of Chapman-Enskog method

-Mass density
$$\rho = \frac{p}{\frac{Y_e}{m_e}kT_e + \sum_{j\neq e}\frac{Y_j}{m_j}kT_h}$$

-Effective diffusion coefficient
$$D_j = \frac{1-Y_j}{\sum_{i\neq j}^{N}\frac{x_j}{D_{ij}}}$$

-Electrical conductivity
$$\sigma_e = \frac{e^2}{kT_e}\frac{n_e}{\sum_{j\neq e}^{N} n_j\Delta_{ej}^{(1)}}$$

-Translational thermal conductivity for heavy particles
$$\lambda_h^{tr} = \frac{15}{4}k\sum_{i\neq e}\frac{n_i}{\sum_{j=1}^{N}\xi_{ij}n_j\Delta_{ij}^{(2)}}$$

-Viscosity
$$\eta = \sum_{j=1}^{N}\frac{m_j n_j}{\sum_{j=1}^{N} n_j\Delta_{ij}^{(2)}}$$

-Translational thermal conductivity for electrons
$$\lambda_e^{tr} = \frac{15}{4}k\frac{n_e}{\sum_{j=1}^{N}\xi_{ej}n_j\Delta_{ej}^{(2)}}$$

2D-Temp. distribution by 1T-CE and 2T-NCE methods

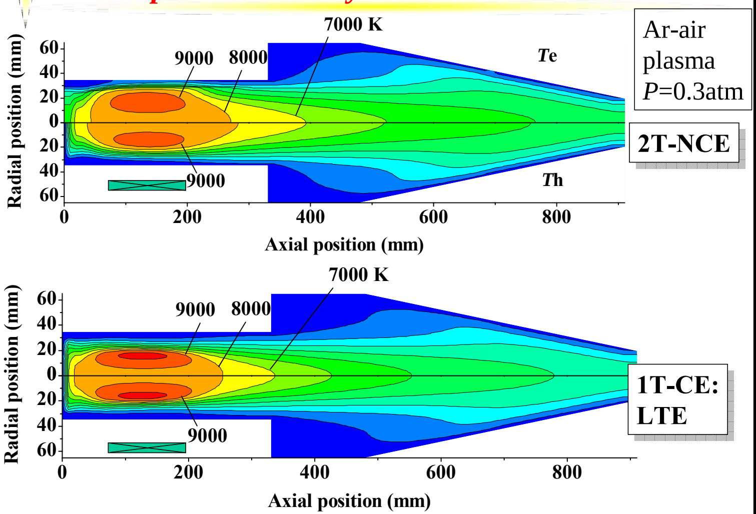

Temperature distribution of Ar-N_2+O_2 & Ar-N_2 plasmas

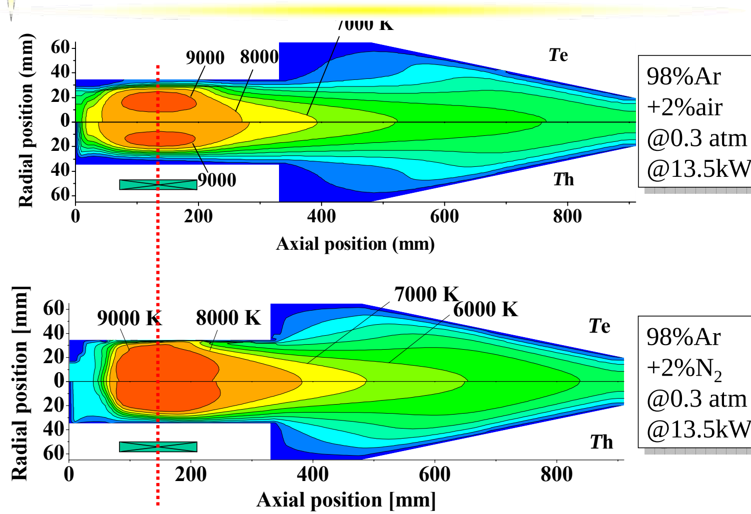

Radial T distribution for Ar-N_2+O_2 & Ar-N_2 plasma

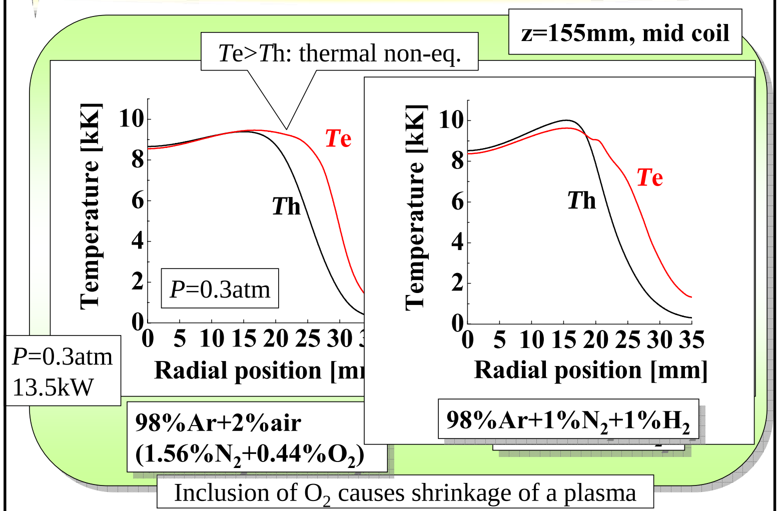

Power balance in Ar-N_2 plasma

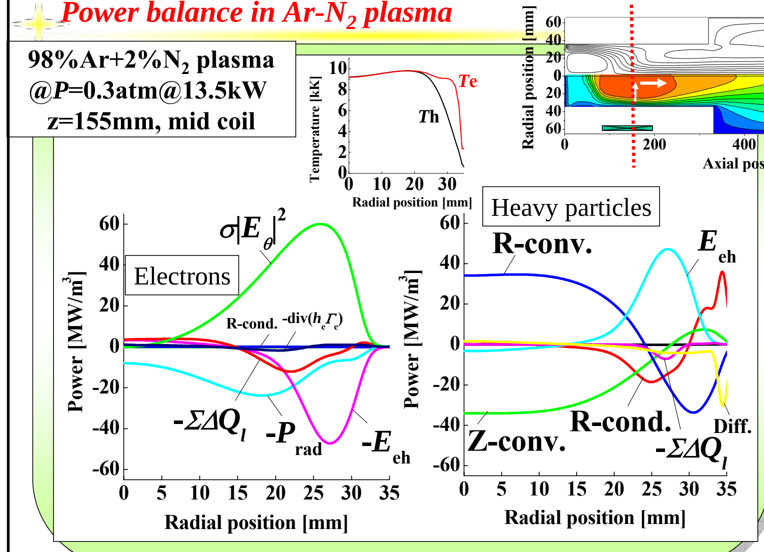

N atom mass fraction by 1T-CE and 2T-NCE methods

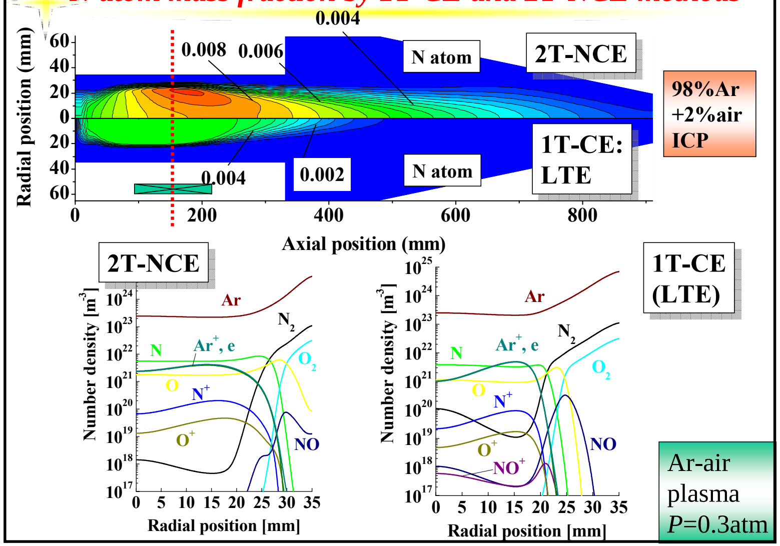

Conclusions

-A 2D-2T-NCE model:

> it was developed for high power argon induction thermal plasmas with molecular gases ($Ar+N_2$, $Ar+N_2+H_2$, $Ar+N_2+O_2$, $Ar+CO_2+H_2$, $Ar+CH_4+O_2$).

-Non-equilibrium effects:

>Thermally and chemically non-equilibrium condition can be seen near the wall in the plasma torch region.

>Non-equilibrium affects prediction of distribution of particle composition.

Future works

- -Full coupling with Boltzmann equation
- -Transport of excited particles
- -Detailed model of radiation transport
- -Separate treatment for electron and ion

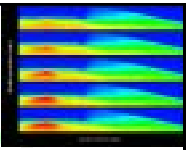

Non-equilibrium modeling of arcs/thermal plasmas

1 *Chemically non-equilibrium effects*

2 *Thermally non-equilibrium effects in ICP*

3 ***Non-Maxwellian EEDF***

Keywords:
- -Non-Maxwellian electron energy distribution function (EEDF)
- -Boltzmann equation
- - Low electron density situation with high electric field strength

---

Introduction → Non-Maxwellian EEDF

Y.Tanaka, JPD, 37, 2004, IEEE DEI, 12, 2005.

Circuit breakers

-There remains a hot gas with temperatures around 3000K after arc interruption.
-Transient recovery voltage(TRV) is applied to the hot gas.

→ **Electrical breakdown can occur through the hot gas.**

For further reliability and compactness of a CB, prediction of dielectric property of hot gas is important for various gases.

GWP of SF_6=23900
→Candidates (SF_6 mixed gas, N_2,CF_3I, CO_2, Air)

The present work

Dielectric properties of hot gas

Critical electric field strength for hot air, air+Cu, CO_2, SF_6 at 300-3500K
→Equilibrium composition calc.+Boltzmann eq.

Non-Maxwellian EEDF

Procedure on prediction of dielectric strength of hot gas

Target:	**Gas kind**	**SF_6, Air, CO_2, Air+Cu**
	Temperature	**300-3500K**
	Electric field	**Uniform**

Particle compositions (ex. equilibrium composition) of hot gases are calculated.

↓

Calculation of effective ionization coefficient $\bar{\alpha}=\alpha-\eta$ of hot gases by solving Boltzmann equation using electron impact cross-section & composition data.

↓

Estimation of critical electric field, which gives $\bar{\alpha}=\alpha-\eta=0$, at different gas temperatures.

Equilibrium composition of 99%Air+1%Cu at 1.0 atm

Dominant particles: N_2, O_2, NO, N_2O, N, O, Cu(cr,*l*), Cu(g), Cu^+, e

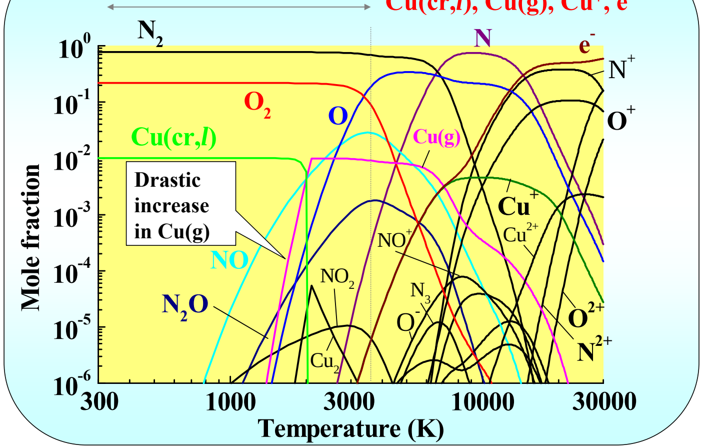

Calculation of effective ionization coefficient

Effective ionization coefficient

$$\frac{\bar{\alpha}}{N} = \frac{\alpha-\eta}{N} = \frac{1}{\upsilon_d}\sum_s \delta_s \left(\frac{2e}{m}\right)^{1/2}\int_0^\infty \sigma_{ioni}(\varepsilon) f(\varepsilon)\,d\varepsilon - \frac{1}{\upsilon_d}\sum_s\delta_s\left(\frac{2e}{m}\right)^{1/2}\int_0^\infty \sigma_{attach}(\varepsilon)f(\varepsilon)\,d\varepsilon$$

Two-term expansion of 0-D Boltzmann eq.

$$\frac{\partial n(\varepsilon)}{\partial t} = -\frac{\partial J_f}{\partial \varepsilon} - \frac{\partial J_{el}}{\partial \varepsilon} + \sum_{s,j} N_s^0 \int_\varepsilon^{\varepsilon+\varepsilon_{sj}} \frac{\partial R_{sj}(\varepsilon) n(\varepsilon)}{\partial \varepsilon}\,d\varepsilon + \left(\frac{\partial n}{\partial \varepsilon}\right)_{e-e}$$

Electron-electron collision term

$$J_f = \frac{2Ne^2(E/N)^2\varepsilon}{3m(2\varepsilon/m)^{1/2}\sum_s \delta_s \sigma_s(\varepsilon)}\left(\frac{n}{2\varepsilon} - \frac{\partial n}{\partial \varepsilon}\right)$$

: Energy gain by electron by E

$$J_{el} = -N\left(\frac{2\varepsilon}{m}\right)^{1/2}\sum_s \delta_s \frac{2m}{M_2}\sigma_e(\varepsilon)\left[n\left(\frac{kT_g}{2} - \varepsilon\right) - kT_g \varepsilon \frac{\partial n}{\partial \varepsilon}\right]$$

: Energy loss in elastic collisions

$$R_{sj}(\varepsilon) = \left(\frac{2}{m}\right)^{1/2}\left[\varepsilon^{1/2}\sigma_{sj}(\varepsilon)\right]$$

Rate of inelastic collisions such as excitation, ionization

$n(\varepsilon) = n_e f_0(\varepsilon)\varepsilon^{1/2}$ **EEDF: Electron Energy Distribution Function**

Electron-ion collisions and electron-electron collisions

Electron-ion collisions

$$\sigma_s^{i}(\varepsilon) \rightarrow (1-\delta_s^{i})\sigma_s^{i}(\varepsilon) + \delta_s^{i}\sigma_{ei}(\varepsilon)$$

$$\sigma_{ei} = 4\pi \frac{e^4}{\varepsilon^2}\ln\Lambda$$ (Coulomb cross section)

Electron-electron collisions

$$\left(\frac{\partial n}{\partial t}\right)_{e-e} = \alpha\left[\frac{3}{\varepsilon^{1/2}}n^2 + 2\varepsilon^{3/2}\frac{\partial \varphi}{\partial \varepsilon}\frac{\partial}{\partial \varepsilon}\left(\frac{\partial n}{\partial \varepsilon} - \frac{n}{2\varepsilon}\right) + \frac{\varphi}{\varepsilon^{1/2}}\left(\frac{\partial n}{\partial \varepsilon} - \frac{n}{2\varepsilon}\right)\right]$$

Obtained by solving the Fokker-Planck equation using the Rosenbluth potentials

Electron impact cross sections for Air+Cu

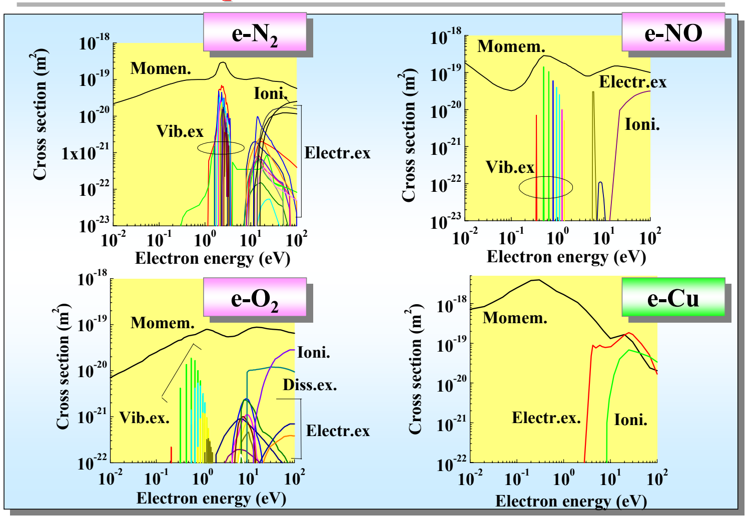

Effective ionization coefficient vs *E/N* and T_g

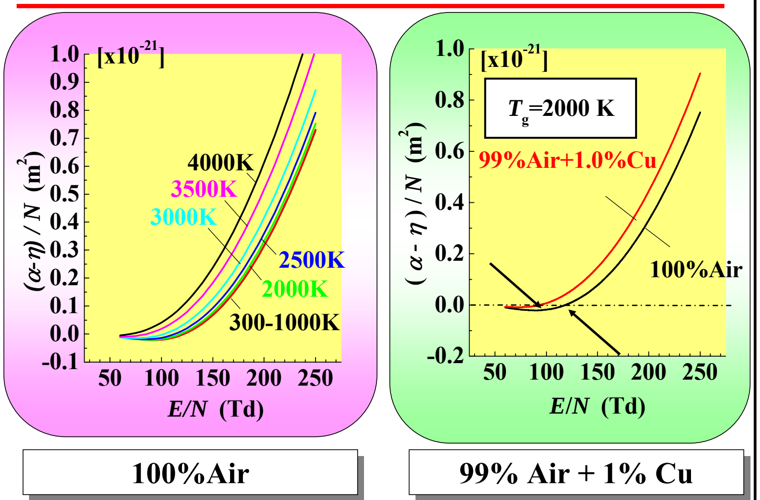

Critical electric field strength of air vs T_g

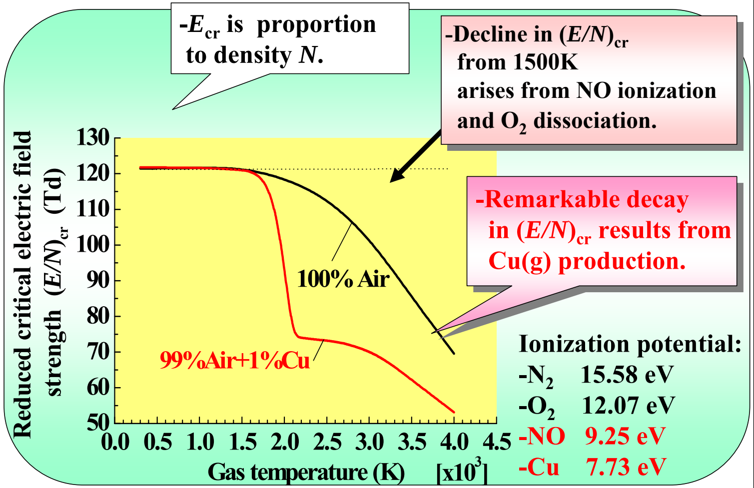

Comparison of critical electric field strength vs T_g

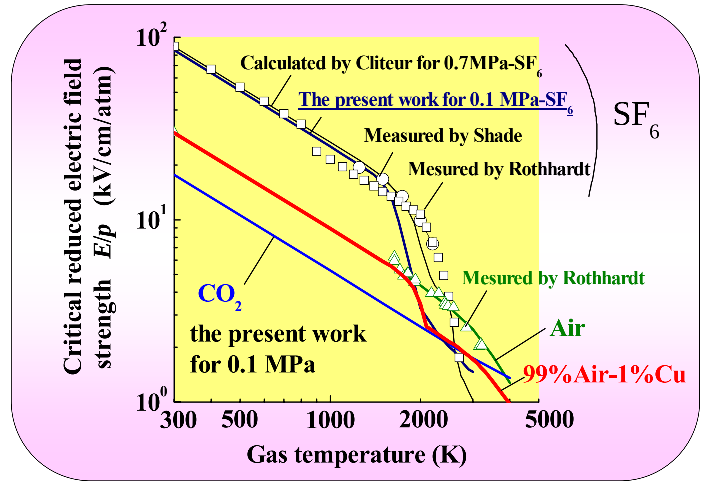

Summary

<Non-equilibrium model in high-T & high-P plasmas>

-Chemically non-equilibrium effect:
→ It can affect the prediction of particle composition and also temperature, in particular, around the fringe of plasmas.

-Thermally non-equilibrium effect : $Te>Th$
→ $Te>Th$ can be seen around the fringe of plasmas. It also affects particle composition there for thermal plasmas.

-Non-Maxwell EEDF: Hot gas to which electric field applied
→ Dielectric strength of hot gas can be predicted by Boltzmann equation solution with high-temperature composition.

Non-equilibrium models should be adopted for advanced understanding of thermal plasmas/arc plasmas.